Pseudouridine-mediated stop codon readthrough in *S. cerevisiae* is sequence context–independent

HIRONORI ADACHI and YI-TAO YU

Department of Biochemistry and Biophysics, Center for RNA Biology, University of Rochester Medical Center, Rochester, New York 14642, USA

ABSTRACT

We have previously shown that when the uridine of a stop codon (UAA, UAG, or UGA) is pseudouridylated, the ribosome reads through the modified stop codon. However, it is not clear as to whether or not the pseudouridine (Ψ)-mediated readthrough is dependent on the sequence context of mRNA. Here, we use several different approaches and the yeast system to address this question. We show that when a stop codon (premature termination codon, PTC) is introduced into the coding region of a reporter mRNA at several different positions (with different sequence contexts) and pseudouridylated, we detect similar levels of readthrough. Using mutational and selection/screen analyses, we also show that the upstream sequence (relative to PTC) as well as the nucleotides surrounding the PTC (upstream and downstream) play a minimal role (if at all) in Ψ-mediated ribosome readthrough. Interestingly, we detect no suppression of NMD (nonsense-mediated mRNA decay) by targeted PTC pseudouridylation in the yeast system. Our results indicate that Ψ-mediated nonsense suppression occurs at the translational level, and that the suppression is sequence context-independent, unlike some previously characterized rare stop codon readthrough events.

Keywords: PTC; pseudouridylation; nonsense suppression; sequence context; stop codon

INTRODUCTION

Termination of protein synthesis occurs when the translating ribosome meets a stop codon (UAA, UAG, or UGA). The encounter between the ribosome and the stop codon triggers a release factor (rather than a charged tRNA) to enter the ribosome and recognize the stop codon, resulting in termination of translation and release of the polypeptide (Dabrowski et al. 2015).

Translation termination occurs not only at the normal stop codon present in each protein-coding gene, but also at the premature termination codon (PTC) resulting from nonsense mutations (from sense codon to nonsense/stop codon) in some genes. In the latter case, PTC often triggers the nonsense-mediated mRNA decay (NMD) pathway, an mRNA quality control surveillance mechanism that degrades the PTC-bearing mRNA (Kurosaki et al. 2019). A small fraction of the mRNA that escapes from NMD degradation is translated but the translation terminates prematurely at the PTC, generating a truncated protein, which is usually nonfunctional and sometimes even harmful to cells. It is now known that a number of known diseases, including some patients suffering from cystic fibrosis, Hurler syndrome, spinal muscular atrophy, and cancer, etc., are due to a nonsense mutation in the disease-causing genes (Gunn et al. 2014; Shimizu-Motohashi et al. 2016; Popp and Maquat 2018; Pranke et al. 2019; Pawlicka et al. 2020). Nonsense suppression, which restores, to some extent, mRNA level and allows the ribosome and tRNA to readthrough the PTC to generate full-length protein, is therefore a highly attractive approach for combating these diseases (Keeling and Bedwell 2011; Peltz et al. 2013; Oren et al. 2017).

We have previously shown that pseudouridylation at a PTC (changing UAA, UAG, or UGA to ΨAA, ΨAG, or ΨGA, respectively) results in PTC readthrough, generating full-length protein (Karijolich and Yu 2011). Based on LC-MS-MS data, both ΨAA and ΨAG code for Ser and Thr, and ΨGA codes for Tyr and Phe. It appears that pseudouridylated stop codons (Ψ-containing PTCs) are no longer normal stop codons; they become sense codons upon pseudouridylation. The crystal structures of ΨAG-bound 30S and 70S ribosomes (bacterial) have been solved (Fernández et al. 2013). According to the structure, Ψ appears to allow or perhaps promote unusual base-pairing

Corresponding author: yitao_yu@urmc.rochester.edu

Article is online at http://www.rnajournal.org/cgi/doi/10.1261/rna.076042.120.

interactions between the pseudouridylated stop codon and its "cognate" tRNA anticodon in the ribosome decoding center. It is likely that the unusual base-pairing makes the codon–anticodon interaction stable enough to allow translation to proceed. Interestingly, it appears that Ψ-mediated nonsense suppression occurs primarily at the translational level (translation termination suppression) rather than at the level of mRNA stability (suppression of NMD) (Karijolich and Yu 2011).

In eukaryotes, RNA pseudouridylation (rRNA and snRNA pseudouridylation in particular) is catalyzed by box H/ACA RNPs, each of which consists of one unique guide RNA (box H/ACA RNA) and four core proteins (Ganot et al. 1997; Rajan et al. 2019). We have shown that by changing the guide sequence of the guide RNA, we can redirect/retarget pseudouridylation to a specific PTC site within an mRNA, leading to nonsense suppression (Huang et al. 2011; Karijolich and Yu 2011). As a potential therapeutic strategy, therefore, targeted mRNA pseudouridylation could potentially be further developed to treat diseases resulting from nonsense mutations (Karijolich and Yu 2014). While this is exciting, one important question remains: Does this Ψ-mediated stop codon readthrough occur in a sequence context-dependent manner?

Here, using the yeast system, we show that Ψ-mediated PTC readthrough occurs even when the PTC is placed at different sites within an mRNA, as long as it is pseudouridylated. We also show that the upstream sequence as well as the nucleotides immediately surrounding the PTC have no obvious effect on pseudouridylated PTC readthrough. Thus, we argue that Ψ-mediated stop codon readthrough is not a rare event that can only occur in some specific sequence context. Pseudouridylated stop codons appear to be "normal" sense codons.

RESULTS

Ψ-mediated PTC readthrough occurs regardless of where the PTC is placed within the coding region of a gene

To test whether or not Ψ-mediated stop codon readthrough is sequence context-dependent, we first moved the PTC randomly along the *TRM4* mRNA, which was used in our previous work (Karijolich and Yu 2011). Using site-directed mutagenesis, we created three carboxy-terminally tagged mutant *TRM4* genes, PTC561 (A561X), PTC602 (F602X), and PTC646 (D646X), each of which contained a PTC (either TAA, TAG, or TGA) at codon 561, codon 602 or codon 646, respectively. These three codon sites are in completely different sequence contexts (Fig. 1A). Designer box H/ACA RNAs, derived from *snR81* RNA

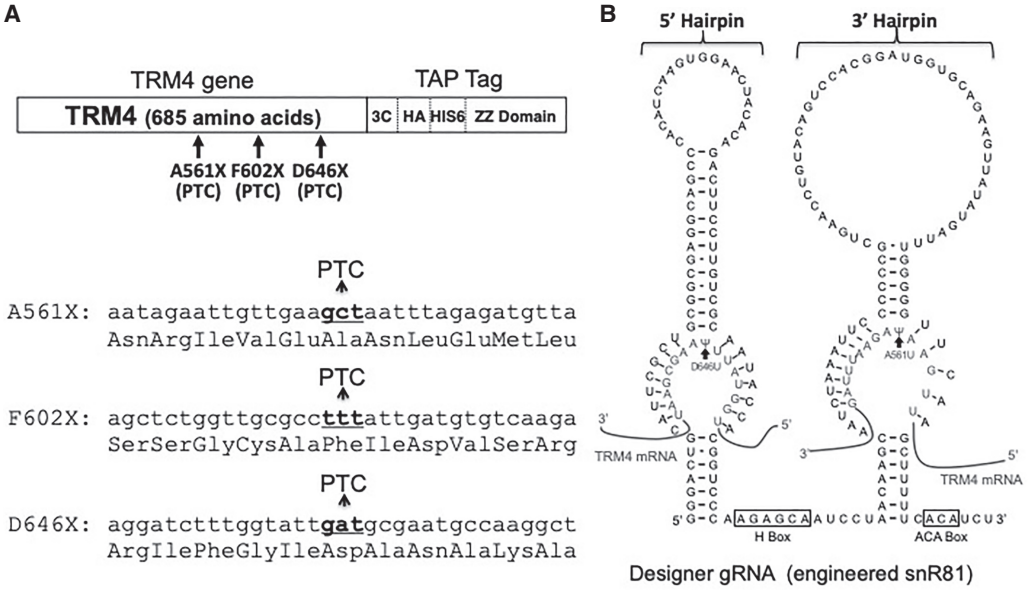

FIGURE 1. Sequence and structure of *TRM4* reporter gene and *snR81*-derived box H/ACA gRNA. (*A*) *TRM4* reporter gene. The carboxy-terminally TAP tagged Trm4 reporter gene is diagrammed (*top*). Three sites (codons 561, 602 and 646) that were targeted for nonsense mutation (mutated to PTC) are indicated. The sequences surrounding the PTC sites are also shown (*bottom*). The DNA sequences are depicted in lower case letters. The target codons (that were changed to PTC) are in bold letters. The amino acid sequences are shown *below* each DNA sequence. (*B*) Sequence and structure of a box H/ACA RNA. Shown is the designer box H/ACA gRNA derived from *snR81* (a naturally occurring yeast box H/ACA RNA). In the designer gRNA, the 5′ pseudouridylation pocket was designed to target the uridine of PTC646 (UAA/UGA), and the 3′ pocket was targeting the uridine of PTC561 (UAG). The two hairpins (5′ and 3′ hairpins) as well as box H and box ACA are indicated. Base-pairing interactions between the guide sequences and the substrate sequences are also depicted. The two arrows indicate the target uridines. The 5′ and 3′ pockets work independently, and they direct U-to-Ψ conversion with essentially the same efficiency.

(only the guide sequences at the pseudouridylation pocket were altered according to the PTC site sequences), were also created for each of these PTCs (Fig. 1B). The efficiency of PTC readthrough was subsequently analyzed (Fig. 2). Briefly, after cotransformation with a *TRM4* construct and a designer box H/ACA RNA construct, yeast cells were lysed and protein isolated. Western blotting (using antibodies against the carboxy-terminal TAP tags, which are located downstream from the PTC sites, see Fig. 1) was subsequently performed. When any of the PTC-containing mutants was cotransformed with a nonspecific (control) box H/ACA RNA, no PTC readthrough product (or a background level of readthrough) was detected (Fig. 2A, lanes 1–3). In contrast, when the PTC-containing mutants were cotransformed with their matching designer box H/ACA RNAs (specific for the PTCs), a clear PTC readthrough product was detected (Fig. 2A, Lanes 4–12). Importantly, for a given PTC (either UAA, UAG, or UGA), we observed strong readthrough signals at the three different sites (with slight differences where site 602 seemed a little higher) (Fig. 2B), suggesting that location or sequence context of the PTC is essentially irrelevant to readthrough. While pseudouridylation at UAG and UGA (converting them to ΨAG and ΨGA, respectively) resulted in a similar level of readthrough products, conversion of UAA to ΨAA appeared to be slightly less efficient in promoting readthrough (Fig. 2B).

Although the NMD effect should also be taken into account when assessing nonsense suppression, we previously showed that there was only a negligible NMD suppression in the yeast system when Ψ was introduced into a PTC by targeted pseudouridylation (Karijolich and Yu 2011). In the current work, we indeed detected virtually no differences in *TRM4* mRNA levels in yeast cells after cotransformation of PTC-containing *TRM4* constructs with specific or nonspecific designer box H/ACA RNAs; *TRM4* mRNA levels were essentially unchanged across all samples (Fig. 3). Likewise, we also detected similar expression levels of various designer box H/ACA RNAs (Fig. 3).

Given that site-specific pseudouridylation is critical for nonsense suppression observed here, and that the UAG-PTC can be efficiently suppressed (Fig. 2), we next decided to measure and compare the pseudouridylation levels of the UAG-containing mRNA at the three test sites, codons 561, 602, and 646. However, the low abundance of mRNA poses a challenge to quantitatively detect Ψ in mRNA using standard pseudouridylation assays. To address this issue, we used a modified pseudouridylation assay, namely, carbodiimide (CMC)-modification followed by reverse transcription-polymerase chain reaction (RT-PCR) (with one upstream primer and one downstream primer, relative to the target uridine site). It is known that Ψ is efficiently modified by CMC, leading to the production of Ψ-CMC adduct, which can quantitatively block RT. Therefore, PCR product level inversely correlates with pseudouridylation level. As shown in Figure 4, it appeared that all three sites were efficiently modified, as low levels of PCR products were generated (Fig. 4A, lanes 7–8, 11–12, and 15–16). Interestingly, slight differences in pseudouridylation levels were also identified at the three sites; a notable higher level of pseudouridylation was observed at codon 602 (F602X) as compared to the other two sites (codon 561 and codon 646) (a lower PCR product was observed) (Fig. 4B, right panel). This observation could perhaps explain why we observed a higher PTC readthrough signal when the F602X constructs were used (Fig. 2).

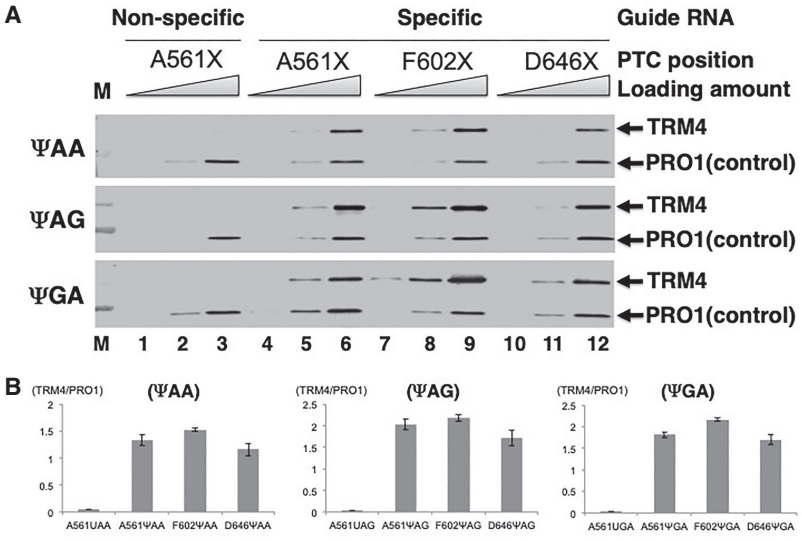

FIGURE 2. Ψ-mediated nonsense suppression using *TRM4* reporter containing a PTC at different sites. (*A*) Western blot analysis. Total proteins were isolated from cells cotransformed with a *TRM4* reporter construct containing a PTC (either UAA, *top* panel; UAG, *middle* panel; and UGA, *bottom* panel) at codon 561 (lanes *1–6*), codon 602 (lanes *7–9*), or codon 646 (lanes *10–12*) and the PTC-specific designer guide RNA (lanes *4–12*) or a nonspecific guide RNA (lanes *1–3*). After immunoprecipitation with antibody against protein A (part of the TAP tag at the carboxyl termini of Trm4 and Pro1), the proteins were resolved on SDS-PAGE, blotted, and probed with anti-Protein A antibody. The Trm4 PTC readthrough protein and the control protein (Pro1) are indicated. Loading amount was titrated in each lane (indicated). Modified PTCs (ΨAA, ΨAG, and ΨGA) are indicated on the *left* (but for the control, lanes *1–3*, the PTCs remain unpseudouridylated). (*B*) Quantification of the western blot shown in *A*. The Trm4 signal was normalized against the signal of Pro1 (control) in each lane, and the quantification results are shown in three panels. (*Left* panel) UAA readthroughs (UAA at three different sites, 561, 602, and 646); (*middle* panel) UAG readthroughs (UAG at positions 561, 602, and 646); (*right* panel) UGA readthroughs (UGA at positions 561, 602, and 646).

Taken together, our results suggest that as long as it is pseudouridylated, the stop codon is read equally well by the ribosome/tRNA, or in other words, Ψ-mediated translational stop codon readthrough or nonsense suppression at the translational level is likely sequence context-independent.

The downstream fourth (+4) nt (relative to the uridine of the PTC) virtually has no effect on PTC readthrough

It has been reported that a short downstream flanking sequence, especially the identity of the fourth (+4) nt (relative to the uridine [+1] of a stop codon) is crucial in influencing rare stop codon readthrough, which occurs during translation of some mRNAs (Li and Rice 1993; Bonetti et al. 1995; McCaughan et al. 1995; Tate et al. 1996; Mao et al. 2004; Loughran et al. 2014; Wei and Xia 2017; Cridge et al. 2018; Yu et al. 2019; Wangen and Green 2020). However, according to published work, the impact of the fourth nucleotide on stop codon readthrough is not entirely consistent. For instance, it appears that in yeast the readthrough efficiency is higher when the fourth (+4) nt immediately following UAG is G or C as compared to A or U (Bonetti et al. 1995). Using a cell-free system, McCaughan et al. (1995) demonstrated that the efficiency of UAG stop codon readthrough is higher when the +4 nt is a pyrimidine (C or U) as compared to a purine (G or A). Recently, it has also been reported that the +4 nt has an impact on geneticin (G418)-mediated stop codon readthrough. Placement of C (or U) at the +4 position results in the highest score in facilitating UAG readthrough (Wangen and Green 2020).

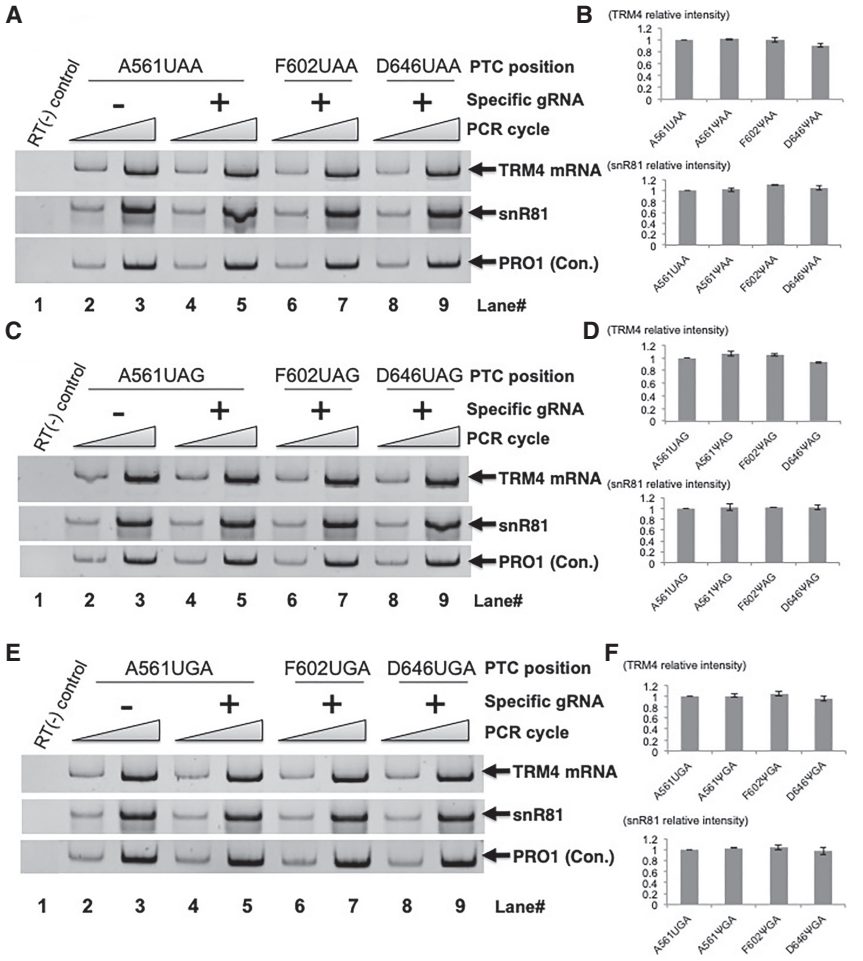

FIGURE 3. Quantitation of RNA levels. (*A*) Total RNA was isolated from cells cotransformed with a *TRM4* reporter construct containing a UAA at codon 561 (lanes *2*–*5*), codon 602 (lanes *6* and *7*), or codon 646 (lanes *8*,*9*) and a PTC-specific designer guide RNA (lanes *4*–*9*) or a nonspecific guide RNA (lanes *2*,*3*). RT-PCR was then carried out (lanes *2*–*9*). A control, PCR without RT, was also shown (lane *1*). The bands of *TRM4*, designer box H/ACA gRNA (derived from *snR81*) and *PRO1* are indicated. (*B*) Quantification of the RT-PCR experiments shown in *A*. (*Top* panel) *TRM4* signal was normalized against the signal of *PRO1* in each lane, and then compared with the control of nonspecific gRNA sample (set as 1) where the uridine of the PTC was not converted to Ψ. (*Bottom* panel) The designer gRNA level was quantified as in the *top* panel (*TRM4* quantification). (*C*) As in *A*, except that the PTC is UAG. (*D*) Quantitation of the experiments shown in *C*. Quantification was carried out exactly as in *B*. (*E*) As in *A*, except that the PTC is UGA. (*F*) Quantitation of the experiments shown in *E*. Quantification was carried out exactly as in *B*.

To determine whether Ψ-mediated stop codon readthrough is similar to or different from the previously reported rare stop codon readthrough, we tested the fourth nucleotide effect using the A561X (UAG) *TRM4* construct. We carried out site-directed mutagenesis and obtained all four +4 A561X *TRM4* constructs each with a different nucleotide (A, C, G, or U) at the forth position (UAGA, UAGC, UAGG, and UAGU). In addition, for each of the +4 A561X *TRM4* constructs we also generated a matching designer box H/ACA RNA targeting the U of the UAG stop codon. Upon cotransformation of a +4 A561X *TRM4* reporter and its matching designer box H/ACA RNA, cells were lysed, and western blotting was carried out. As shown in Figure 5, the Ψ-mediated UAG readthrough efficiency appeared to be similar (although not identical) for the four constructs. The efficiency was slightly higher when the fourth position nucleotide was a G. Although not the best, A, when placed at the fourth position, appeared to be slightly better than C or U in facilitating UAG readthrough. These results were clearly

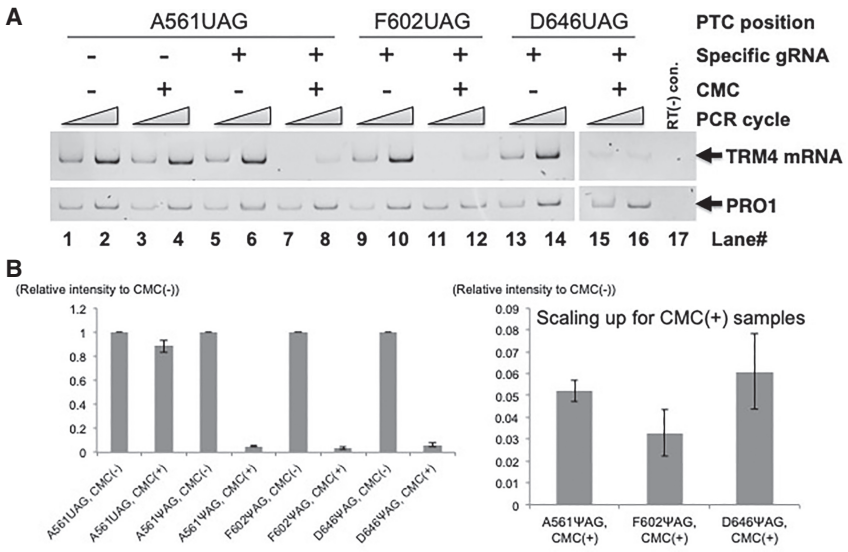

FIGURE 4. Quantification of mRNA pseudouridylation. (*A*) Total RNA was extracted from cells cotransformed with the *TRM4* reporter construct containing a PTC (UAG) at codon 561 (lanes *1–8*), codon 602 (lanes *9–12*), or codon 646 (lanes *13–16*) and the PTC-specific designer guide RNA (lanes *5–16*) or a nonspecific guide RNA (lanes *1–4*), and treated with CMC [N-cyclohexyl-N′-b-(4-methylmorpholinium) ethylcarbodiimide] (lanes *3*,*4*,*7*,*8*,*11*,*12*,*15*,*16*) or buffer (lanes *1*,*2*,*5*,*6*,*9*,*10*,*13*,*14*). After hydrolysis with alkaline, the RNA samples were then used for RT with a primer complementary to a sequence at the 5′ end of the TAP tag sequence. PCR was then carried out, using a forward primer corresponding to an upstream sequence (relative to the target uridine) and a reverse primer complementary to a downstream sequence (relative to the target uridine). In each reaction, a different set of PCR primers was also included to measure the level of *PRO1* mRNA (as a control). The positions of *TRM4* and *PRO1* are indicated. Lane *17* is a control (PCR without RT). (*B*) Quantitation of the experiments shown in *A*. (*Left* panel) The *TRM4* signal was normalized against the *PRO1* signal in each lane. CMC-plus samples were then compared with the CMC-minus samples (which are set as 1). (*Right* panel) Amplification of the three samples shown in the *left* panel, A561ΨAG CMC(+), A602ΨAG CMC(+), and A646ΨAG CMC(+). The signal intensity (*Y*-axis) inversely correlates to pseudouridylation level. We estimate that the level of pseudouridylation at every target site (in the presence of site-specific gRNA) is ∼10%–15%.

different from previously published data on rare stop codon readthrough.

Thus, our results suggest that Ψ-mediated stop codon readthrough is different from rare stop codon readthrough previously reported (Bonetti et al. 1995; McCaughan et al. 1995; Wangen and Green 2020) and that pseudouridylated stop codons (at least for UAG) behave more like regular sense codons.

The −1 nt (immediately 5′ adjacent to the PTC) has no effect on PTC readthrough

Having determined that the forth nucleotide had no obvious effect on Ψ-mediated UAG stop codon readthrough, we next tested whether the −1 nt (relative to the +1 uridine of the PTC), which was also reported to have influence on rare stop condon readthrough (Cassan and Rousset 2001), had an impact on Ψ-mediated stop codon readthrough. Using site-directed mutagenesis, we generated all four −1 A561X (UAG) PTC *TRM4* constructs, each with a different nucleotide (A, U, C, or G) at the −1 nt position (AUAG, CUAG, GUAC, and UUAG). Designer box H/ACA RNAs specifically targeting the U of PTC (UAG) were also generated. Upon cotransformation of the reporter and the matching designer box H/ACA RNA constructs, western analysis was carried out. As shown in Figure 6, no or little difference in readthrough levels was observed among the four −1 A561X (ΨAG) constructs.

RT-PCR analysis indicated that all four *TRM4* constructs were expressed at a similar level. The same was true for the designer box H/ACA RNAs (Fig. 7).

Taken together, the nucleotide immediately preceding the UAG stop codon showed no or little impact on Ψ-mediated UAG stop codon readthrough, suggesting again that Ψ-mediated stop codon readthrough is different from the previously reported rare stop codon readthrough.

Screen of upstream sequence (5′ adjacent to PTC) shows no sequence preference during Ψ-mediated stop codon readthrough

To further examine the possible sequence preference, we took advantage of the box H/ACA RNA-guided pseudouridylation mechanism in which the guide sequences on both sides (5′- and 3′-sides) of the pseudouridylation pocket form stable enough base-pairing interactions with the substrate sequences (flanking the target U) (see Figs. 1B, 8B). Specifically, the substrate sequence immediately upstream of (5′ of) the target U base-pairs with the 3′-side guide sequence (3′-side of the pseudouridylation pocket), and the substrate sequence downstream from (3′ of) the target U pairs with the 5′-side guide sequence (5′ side of the pseudouridylation pocket) (Fig. 8B). It is known that base pairs between the guide RNA and its substrate are rather flexible. In fact, the numbers of base pairs on the 5′ and 3′ sides of the pseudouridylation pocket can but do not have to be identical (De Zoysa et al. 2018). For instance, the number of base pairs on one side could be much bigger than that on the other side as long as the overall base-pairing between the guide and the substrate is sufficiently stable. In other words, a small number (the limit is two) of base pairs (unstable interactions) on one side can be compensated by more base pairs (more stable interactions) on the other side.

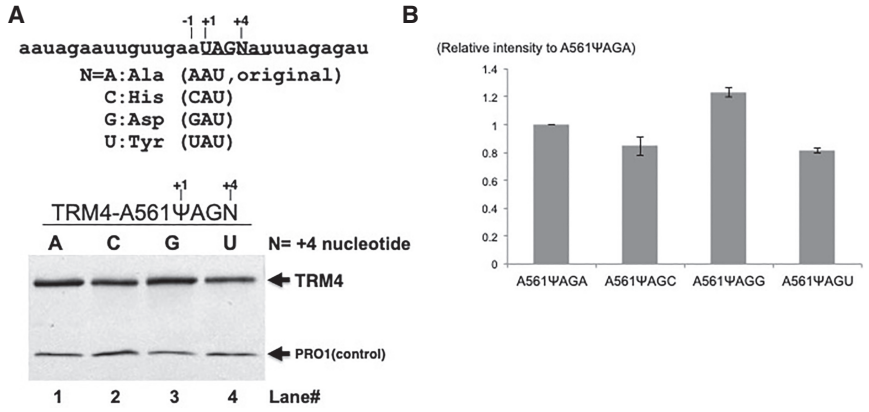

FIGURE 5. Measurement of the effect of +4 nt on Ψ-mediated nonsense suppression. (*A*) Western blot analysis. Total proteins were isolated from cells cotransformed with two constructs: (1) A *TRM4* reporter construct, where a PTC (TAG, or UAG in RNA) was placed at codon 561 and the +4 nt (relative to the uridine of PTC) was A (lane *1*; original sequence), or changed to C (lane *2*), G (lane *3*), or T (or U in RNA) (lane *4*), and (2) a PTC-specific designer guide RNA (lanes *1*–*4*). After immunoprecipitation with antibody against protein A (part of the TAP tag at the C-termini of Trm4 and Pro1), the proteins were resolved on SDS-PAGE, blotted, and probed with anti-Protein A antibody. The Trm4 PTC readthrough protein and the control protein (Pro1) are indicated. The RNA sequence surrounding the PTC (UAG at codon 561) is also shown (*top*). Capital letters indicate the PTC stop codon and N represents the +4 nt, which can be either A, C, G or U. +1 and +4 nt are indicated. *Below* the RNA sequence are the four possible codons when +4 nucleotide (N) is changed to A, C, G, or U, and the amino acids they code for. (*B*) Quantitation of the experiments shown in *A*. The intensity of Trm4 signal is normalized against Pro1 signal in the same lane and compared with the signal (set as 1) of the original construct where +4 nt is *A* (lane *1* in *A*).

Based on the above rule, we designed a box H/ACA guide RNA that forms only two guide-substrate base pairs on the 3′ side of the pocket, and 10 guide-substrate base pairs on the 5′ side of the pocket (to compensate the unstable 3′ side). Ten nucleotides of substrate sequence, located 2 nt upstream of the target U (from −3 to −12 relative to target U site) (Fig. 8A,B), were then randomized. It has also been demonstrated that a total of 8 bp (between the guide and the substrate) are sufficient for efficient pseudouridylation (De Zoysa et al. 2018; Kelly et al. 2019). In other words, modification efficiency does not significantly improve with increasing number (more than eight) of base pairs between the guide and substrate. Therefore, even if the randomized nucleotides are minimally involved in pairing with the 3′ side of the guide sequence, this arrangement would presumably allow each substrate (with any sequence from −3 to −12) to be equally pseudouridylated at the target U (assuming the substrate sequences, 2 nt at positions −1 and −2, and 10 nt from +3 to position +12, are always available for pairing with the guide sequence), thus enabling us to test, in an unbiased way, whether there is a sequence preference in this region (from site −3 to site −12).

We obtained a large number of yeast cell colonies after cotransformation of the randomized (nts from −3 to −12) PTC-containing *TRM4* (A561X UAG) and its specific designer box H/ACA guide RNA. We isolated 30 colonies and tested some of them for PTC readthrough efficiency using western analysis. Except for some that showed no readthrough (Fig. 8C, lanes 3 and 5), all the others exhibited similar levels of PTC readthrough (Fig. 8C, lanes 1, 2, 4, 6, and 7). To know the exact sequence from site −3 to site −12, plasmids were recovered from these cells and sequenced (Fig. 8D). The sequencing results indicated that the two that showed no

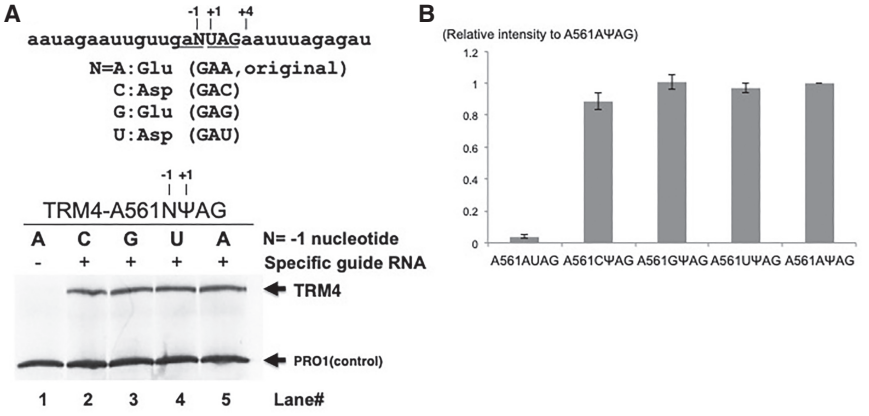

FIGURE 6. Measurement of the effect of −1 nt on Ψ-mediated nonsense suppression. (*A*) Western blot analysis. Total proteins were isolated from cells cotransformed with two constructs: (1) A *TRM4* reporter construct, where a PTC (TAG, or UAG in RNA) was placed at codon 561 and the −1 nt (relative to the uridine of PTC) was A (lanes *1*,*5*; original sequence), or changed to C (lane *2*), G (lane *3*) or T (or U in RNA) (lane *4*), and (2) a PTC-specific designer guide RNA (lanes *2*–*5*) or a nonspecific designer guide RNA (lane *1*). After immunoprecipitation with antibody against protein A (part of the TAP tag at the carboxyl termini of Trm4 and Pro1), the proteins were resolved on SDS-PAGE, blotted, and probed with anti-Protein A antibody. The Trm4 PTC readthrough protein and the control protein (Pro1) are indicated. The RNA sequence surrounding the PTC (UAG at codon 561) is also shown (*top*). Capital letters indicate the PTC stop codon and N represents the −1 nt, which can be either A, C, G, or U. −1, +1, and +4 nt are indicated. *Below* the RNA sequence are the four possible codons when the −1 nt (N) is changed to A, C, G, or U, and the amino acids they code for. (*B*) Quantitation of the experiments shown in *A*. The intensity of Trm4 signal is normalized against Pro1 signal in the same lane, and compared with the signal (set as 1) of the original construct (the −1 nt is A) cotransformed with the PTC-specific guide RNA (Sample A561AΨAG, lane *5* in *A*).

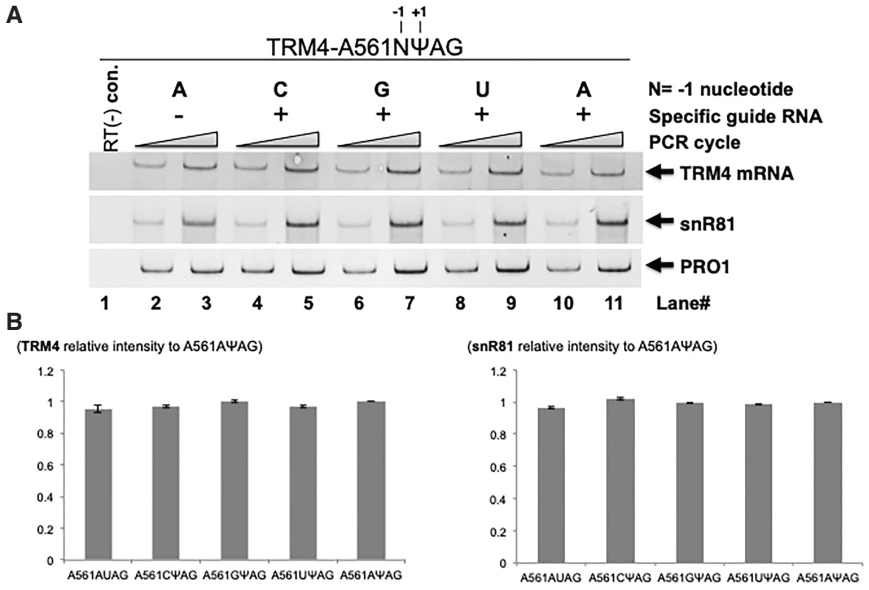

FIGURE 7. Quantitation of RNA levels. (*A*) Total RNA was isolated from cells cotransformed with two constructs: (1) A *TRM4* reporter construct, where a PTC (TAG, or UAG in RNA) was placed at codon 561 and the −1 nt (relative to the uridine of PTC) was changed to either A (lanes *2*,*3*,*10*,*11*), C (lane *4*,*5*), G (lane *6*,*7*), or T (or U in RNA) (lane *8*,*9*), and (2) a PTC-specific designer guide RNA (lanes *4*–*11*) or a nonspecific designer guide RNA (lanes *2*,*3*). RT-PCR was then carried out (lanes *2*–*11*). A control, PCR without RT, was also shown (lane *1*). The bands of *TRM4*, designer box H/ACA gRNA (derived from *snR81*) and *PRO1* are indicated. (*B*) Quantification of the RT-PCR experiments shown in *A*. (*Left* panel) The *TRM4* signal was normalized against the signal of *PRO1* in the same lane, and then compared with the signal of the control—the original construct (the −1 nt is *A*) cotransformed with the PTC-specific guide RNA (Sample A561AΨAG, lanes *10*,*11*) (set as 1). (*Right* panel) The designer gRNA level was quantified as in the *left* panel (*TRM4* quantification).

readthrough (Fig. 8C, lanes 3 and 5) had a stop codon in this region (Fig. 8D, #3 and #5). The others had various sequences that coded for different amino acids. These results, although obtained from a small number of samples/colonies, suggest that the upstream sequence (from −3 to −12 relative to the first nucleotide of PTC) probably has no or little influence on PTC readthrough.

DISCUSSION

While Ψ-mediated stop codon readthrough was discovered several years ago (Karijolich and Yu 2011), it was not clear as to whether or not the sequences surrounding the target stop codon play a role in this translational readthrough event. In the current work, we showed several independent lines of evidence suggesting that the sequence context was irrelevant. First, we placed the PTC at three randomly selected sites within the *TRM4* gene, and found no significant differences in Ψ-mediated PTC readthrough between the three sites, thus suggesting there is no sequence preference for this process. Second, we mutated the +4 and −1 nt, which immediately flank the target stop codon, and tested the effect of the mutations on PTC readthrough. Unlike the natural leaky stop codons that are influenced by the surrounding nucleotides, Ψ-mediated stop codon readthrough appears to be independent of the fourth (+4) or the −1 nt. Third, we randomized a 10 nt sequence 5′ of the PTC (from −3 to −12 relative to the PTC site), and generated a large number of constructs. We observed a similar level of Ψ-mediated PTC readthrough for all constructs tested (with the exception of those that created a new stop codon), suggesting that the sequence 5′ of the target PTC plays no role in PTC readthrough. Taken together, our results suggest that pseudouridylated stop codons behave similarly to normal sense codons.

While no clear sequence context-dependence was detected, the structure of RNA may still be a factor. In other words, the accessibility of the target site, which could be influenced by RNA secondary/tertiary structure, is likely critical for targeted modification. In this regard, protein binding at or near the target site may also interfere with the modification efficiency, and hence may impact PTC readthrough and nonsense suppression.

We showed here that transformation of the PTC-specific designer guide RNA had no effect on steady state levels of PTC-bearing mRNA. Indeed, we detected virtually identical levels of PTC-bearing mRNA regardless of which guide RNA (PTC-specific or nonspecific) was cotransformed (Fig. 3). Our current data are consistent with the results published before, where we demonstrated that nonsense suppression was a result of translation termination suppression rather than a result of suppression of NMD (Karijolich and Yu 2011). Although it is not totally clear at the moment why NMD was not suppressed, we speculate that this phenomenon is unique to yeast (species difference between yeast and mammals). Indeed, it has been reported that the NMD effect in yeast does not appear to be entirely the same as in mammalian cells due at least in part to the fact that most of pre-mRNAs are not spliced in yeast cells (Parenteau et al. 2008). In this regard, the *TRM4* reporter we used in this study does not contain an intron. In addition, it has been demonstrated that while in mammalian cells, NMD is restricted to CBC (cap binding complex)-bound mRNA, yeast NMD occurs minimally on CBC-bound transcripts (Kuperwasser et al. 2004; Rufener

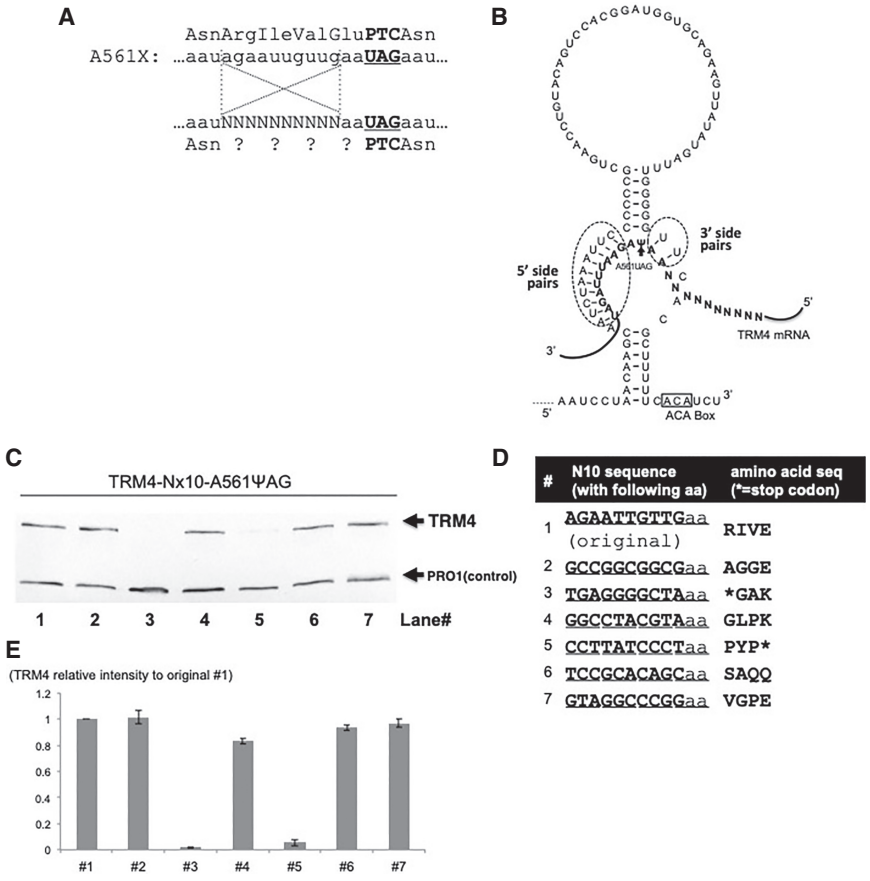

FIGURE 8. The effect of an upstream sequence on Ψ-mediated nonsense suppression. (*A*) A short sequence upstream of the PTC (UAG) at codon 561 (A561X) is shown. *Above* the A561X nucleotide sequence is the amino acid sequence. The bold letters indicate the stop codon 561 (or PTC561). *Below* the A561X nucleotide sequence is a mutant A561X sequence where the 10 nt from −12 to −3 (relative to the uridine [+1] of the PTC) are randomized (Ns), and this mutant sequence was used for screen experiments. *Below* the mutant A561X sequence is the amino acid sequence with question marks representing unknown amino acids (due to the 10 randomized nucleotides within the A561X mRNA). (*B*) The 3′ hairpin of designer box H/ACA gRNA (targeting the uridine of the A561X stop codon) is shown. Also shown are the base-pairing interactions between the guide sequence and the substrate sequence (bold letters). While there are 10 bp on the 5′ side of pseudouridylation pocket (dotted circle), there are only 2 bp on the 3′ side (dotted circle). The 10 randomized nucleotides (Ns) are also shown. (*C*) Western blotting analysis of some representative samples (after screen experiments, see text). Yeast cells were cotransformed with the 10 nt randomized A561X construct (described in *A*) and the PTC-specific designer gRNA (shown in *B*). Several colonies were selected and total proteins were isolated from these individual colonies. Western blotting was carried out exactly as in Fig. 2A. Trm4 and Pro1 were indicated. (*D*) Sequences of the mutant A561X analyzed in *C*. The seven samples tested in *C* were sequenced, and their nucleotide sequences (*left*) as well as amino acid sequences (*right*) are shown. Two of the seven sequences, #3 and #5 corresponding to lanes *3* and *5* in *C*, have a stop codon (asterisks). (*E*) Quantitation of the experiments shown in *C*. The Trm4 signal was normalized against the signal of Pro1 (control) in each lane and compared with the readthrough signal generated from the original (wild-type) sequence (#1) (set as 1).

and Mühlemann 2013). To definitively clarify this issue, it is necessary to carry out a similar experiment analyzing Ψ-mediated nonsense suppression (on both NMD suppression and translation termination suppression) in mammalian cells.

Although no significant difference was observed, we detected some small differences in nonsense suppression levels (final readthrough protein products) when sequences/nucleotides surrounding the PTC were mutated. There are at least three possibilities that could explain these small differences. First, we still cannot completely rule out the possibility that the differences could be a direct result of slightly different efficiencies of translational stop codon readthrough. Second, it is possible that changes of surrounding sequences/nucleotides result in codon changes, which could in turn slightly alter translation elongation rates due to different frequencies of codon usage, thus generating different amounts of readthrough protein product. Finally, we believe that our observed different levels of nonsense suppression are more likely due to the differences in efficiency of stop codon pseudouridylation. Indeed, the pseudouridylation quantitation experiments (Fig. 4) indicated that the level of Ψ was slightly different when PTC was placed at different positions along the *TRM4* reporter gene, and that the difference of pseudouridylation level somewhat correlated with the level of final readthrough protein product. Regardless, despite the small differences in the production of final readthrough products, we conclude that Ψ-mediated translational stop codon readthrough itself is mostly sequence context-independent.

MATERIALS AND METHODS

Yeast strain and plasmids

Parental *S. cerevisiae* strain used in this work was BY4741/*PRO1*-TAP (kindly provided by E. Phizicky). Plasmids used in this work were derived from p*TRM4-GAL*p-F602X [*URA3*, 2μ] and YEplac181-GPDp-*snR81TRM4* [*LEU2*, 2μ] (Karijolich and Yu 2011; Wu et al. 2016). Site-directed mutagenesis was carried out to introduce PTC at A561 and D646. Cloning of each guide RNA expression vector was performed as previously described (Karijolich and Yu 2011; Wu et al. 2016). A nonspecific guide RNA, targeting U2 snRNA U44, was also created. Two

guide RNA sequences are shown in Figures 1B, 8B. All the others, used in this work, are shown in Supplemental Figure 1.

Western blotting

For the analysis of Trm4 PTC readthrough, yeast cell culture, total protein extraction, and immunoprecipitation were carried out as described before (Ma et al. 2005). Briefly, *TRM4* and designer guide RNA cotransformed yeast cells were precultured in SD-Ura-Leu medium. After overnight incubation, cells were collected, washed, and inoculated to raffinose medium and grown to O. D.600 = 0.8. Galactose was then added to induce *GAL* promoter-driven *TRM4* expression. After lysing yeast cells with glass beads, the whole cell extract was applied to IgG Sepharose 6 Fast Flow (GE Healthcare). Immunoprecipitated proteins were eluted by boiling at 95°C for 2 min with Laemmli SDS sample buffer. The eluted proteins were resolved by SDS-PAGE, which was followed by western blotting, where rabbit anti-Protein A (P3775, SIGMA) was used for the first antibody and anti-rabbit IgG-AP Conjugate (170-6518, Bio-Rad) was used for the secondary antibody. The proteins were detected with one-step NBT/BCIP Substrate Solution (34042, Thermo Fisher).

Pseudouridylation assay and RNA measurement

Yeast total RNA was extracted with TRIzol Reagent. First, cell pellets were resuspended with TRIzol Reagent (1 mL of TRIzol Reagent to 50 mL of yeast cells), and cells were lysed by bead beating with 0.5 mm glass beads. Following this step, RNA extraction was carried out as previously described (Adachi et al. 2019). The recovered total RNA was then applied to DNase treatment to remove all genomic and plasmid DNAs. For CMC treatment, a half of the total RNA was incubated with CMC at 37°C for 30 min (the other half was incubated with buffer) and after ethanol precipitation, the RNA was incubated with alkaline buffer at 37°C for 2 h to remove CMC from U and G bases (but Ψ-CMC remains). The total RNA (either CMC treated or untreated) was reverse transcribed with a reverse primer that pairs with the 5′ end sequence of TAP tag (GGACCTTGGAACAAAGCTTC) (Bakin and Ofengand 1993). PCR reaction was then performed with two pairs of primers: Fwd-*TRM4*A561 – 85 (AAGTGATATC GAATGTTCATGG) and Rev-*TRM4*D646 + 20 (GAGATTCAGTCG TTTC) for *TRM4*, and Fwd-*PRO1*(987–1004) (TGCGTACGCAGC CTTAAC) and Rev-*PRO1*(1243–61) (CTCTATGAGCGACATAT TC) for *PRO1*.

To measure RNA levels, RT-PCR was performed directly without CMC modification. The primers for measuring *TRM4* mRNA and *PRO1* mRNA are the same as those described above. For measuring the levels of *snR81*-derived designer guide RNAs, the RT primer is complementary to a designer guide RNA-specific sequence (nt 110–130). The two primers for PCR are Fwd-*snR81* (22–41) (GCGGCGAGGCAGCCCACATC) and Rev-*snR81*(87–103) (GCTTGTTAGGATTGCTC).

Quantification

Quantification was performed by Image Studio Lite (LI-COR Biosciences). It was confirmed that the intensity of the bands to be quantified are in a linear range. The intensity of each band was normalized against the control band (*PRO1*). To show relative intensity, the value of a sample to be compared with was set as 1 (for detail, see figure legends). The error bars indicate ±S.D.

SUPPLEMENTAL MATERIAL

Supplemental material is available for this article.

ACKNOWLEDGMENTS

We thank members of the Yu laboratory for insightful discussions. This work was supported by grant CA241111 from the U.S. National Institutes of Health and grant CFF YU20G0 from the Cystic Fibrosis Foundation.

Received April 23, 2020; accepted May 19, 2020.

REFERENCES

Adachi H, De Zoysa MD, Yu YT. 2019. Detection and quantification of pseudouridine in RNA. *Methods Mol Biol* **1870:** 219–235. doi:10.1007/978-1-4939-8808-2_17

Bakin A, Ofengand J. 1993. Four newly located pseudouridylate residues in *Escherichia coli* 23S ribosomal RNA are all at the peptidyltransferase center: analysis by the application of a new sequencing technique. *Biochemistry* **32:** 9754–9762. doi:10.1021/bi00088a030

Bonetti B, Fu L, Moon J, Bedwell DM. 1995. The efficiency of translation termination is determined by a synergistic interplay between upstream and downstream sequences in *Saccharomyces cerevisiae*. *J Mol Biol* **251:** 334–345. doi:10.1006/jmbi.1995.0438

Cassan M, Rousset JP. 2001. UAG readthrough in mammalian cells: effect of upstream and downstream stop codon contexts reveal different signals. *BMC Mol Biol* **2:** 3. doi:10.1186/1471-2199-2-3

Cridge AG, Crowe-McAuliffe C, Mathew SF, Tate WP. 2018. Eukaryotic translational termination efficiency is influenced by the 3′ nucleotides within the ribosomal mRNA channel. *Nucleic Acids Res* **46:** 1927–1944. doi:10.1093/nar/gkx1315

Dabrowski M, Bukowy-Bieryllo Z, Zietkiewicz E. 2015. Translational readthrough potential of natural termination codons in eucaryotes–The impact of RNA sequence. *RNA Biol* **12:** 950–958. doi:10.1080/15476286.2015.1068497

De Zoysa MD, Wu G, Katz R, Yu YT. 2018. Guide-substrate base-pairing requirement for box H/ACA RNA-guided RNA pseudouridylation. *RNA* **24:** 1106–1117. doi:10.1261/rna.066837.118

Fernández IS, Ng CL, Kelley AC, Wu G, Yu YT, Ramakrishnan V. 2013. Unusual base pairing during the decoding of a stop codon by the ribosome. *Nature* **500:** 107–110. doi:10.1038/nature12302

Ganot P, Bortolin ML, Kiss T. 1997. Site-specific pseudouridine formation in preribosomal RNA is guided by small nucleolar RNAs. *Cell* **89:** 799–809. doi:10.1016/S0092-8674(00)80263-9

Gunn G, Dai Y, Du M, Belakhov V, Kandasamy J, Schoeb TR, Baasov T, Bedwell DM, Keeling KM. 2014. Long-term nonsense suppression therapy moderates MPS I-H disease progression. *Mol Genet Metab* **111:** 374–381. doi:10.1016/j.ymgme.2013.12.007

Huang C, Karijolich J, Yu YT. 2011. Post-transcriptional modification of RNAs by artificial Box H/ACA and Box C/D RNPs. *Methods Mol Biol* **718:** 227–244. doi:10.1007/978-1-61779-018-8_14

Karijolich J, Yu YT. 2011. Converting nonsense codons into sense codons by targeted pseudouridylation. *Nature* **474:** 395–398. doi:10.1038/nature10165

Karijolich J, Yu YT. 2014. Therapeutic suppression of premature termination codons: mechanisms and clinical considerations (review). *Int J Mol Med* **34:** 355–362. doi:10.3892/ijmm.2014.1809

Keeling KM, Bedwell DM. 2011. Suppression of nonsense mutations as a therapeutic approach to treat genetic diseases. *Wiley Interdiscip Rev RNA* **2:** 837–852. doi:10.1002/wrna.95

Kelly EK, Czekay DP, Kothe U. 2019. Base-pairing interactions between substrate RNA and H/ACA guide RNA modulate the kinetics of pseudouridylation, but not the affinity of substrate binding by H/ACA small nucleolar ribonucleoproteins. *RNA* **25:** 1393–1404. doi:10.1261/rna.071043.119

Kuperwasser N, Brogna S, Dower K, Rosbash M. 2004. Nonsense-mediated decay does not occur within the yeast nucleus. *RNA* **10:** 1907–1915. doi:10.1261/rna.7132504

Kurosaki T, Popp MW, Maquat LE. 2019. Quality and quantity control of gene expression by nonsense-mediated mRNA decay. *Nat Rev Mol Cell Biol* **20:** 406–420. doi:10.1038/s41580-019-0126-2

Li G, Rice CM. 1993. The signal for translational readthrough of a UGA codon in Sindbis virus RNA involves a single cytidine residue immediately downstream of the termination codon. *J Virol* **67:** 5062–5067. doi:10.1128/JVI.67.8.5062-5067.1993

Loughran G, Chou MY, Ivanov IP, Jungreis I, Kellis M, Kiran AM, Baranov PV, Atkins JF. 2014. Evidence of efficient stop codon readthrough in four mammalian genes. *Nucleic Acids Res* **42:** 8928–8938. doi:10.1093/nar/gku608

Ma X, Yang C, Alexandrov A, Grayhack EJ, Behm-Ansmant I, Yu YT. 2005. Pseudouridylation of yeast U2 snRNA is catalyzed by either an RNA-guided or RNA-independent mechanism. *EMBO J* **24:** 2403–2413. doi:10.1038/sj.emboj.7600718

Mao PL, Liu TF, Kueh K, Wu P. 2004. Predicting the efficiency of UAG translational stop signal through studies of physicochemical properties of its composite mono- and dinucleotides. *Comput Biol Chem* **28:** 245–256. doi:10.1016/j.compbiolchem.2004.05.003

McCaughan KK, Brown CM, Dalphin ME, Berry MJ, Tate WP. 1995. Translational termination efficiency in mammals is influenced by the base following the stop codon. *Proc Natl Acad Sci* **92:** 5431–5435. doi:10.1073/pnas.92.12.5431

Oren YS, Pranke IM, Kerem B, Sermet-Gaudelus I. 2017. The suppression of premature termination codons and the repair of splicing mutations in CFTR. *Curr Opin Pharmacol* **34:** 125–131. doi:10.1016/j.coph.2017.09.017

Parenteau J, Durand M, Véronneau S, Lacombe AA, Morin G, Guérin V, Cecez B, Gervais-Bird J, Koh CS, Brunelle D, et al. 2008. Deletion of many yeast introns reveals a minority of genes that require splicing for function. *Mol Biol Cell* **19:** 1932–1941. doi:10.1091/mbc.e07-12-1254

Pawlicka K, Kalathiya U, Alfaro J. 2020. Nonsense-mediated mRNA decay: pathologies and the potential for novel therapeutics. *Cancers (Basel)* **12:** E765. doi:10.3390/cancers12030765

Peltz SW, Morsy M, Welch EM, Jacobson A. 2013. Ataluren as an agent for therapeutic nonsense suppression. *Annu Rev Med* **64:** 407–425. doi:10.1146/annurev-med-120611-144851

Popp MW, Maquat LE. 2018. Nonsense-mediated mRNA decay and cancer. *Curr Opin Genet Dev* **48:** 44–50. doi:10.1016/j.gde.2017.10.007

Pranke I, Golec A, Hinzpeter A, Edelman A, Sermet-Gaudelus I. 2019. Emerging therapeutic approaches for cystic fibrosis. From gene editing to personalized medicine. *Front Pharmacol* **10:** 121. doi:10.3389/fphar.2019.00121

Rajan KS, Doniger T, Cohen-Chalamish S, Chen D, Semo O, Aryal S, Glick Saar E, Chikne V, Gerber D, Unger R, et al. 2019. Pseudouridines on *Trypanosoma brucei* spliceosomal small nuclear RNAs and their implication for RNA and protein interactions. *Nucleic Acids Res* **47:** 7633–7647. doi:10.1093/nar/gkz477

Rufener SC, Mühlemann O. 2013. eIF4E-bound mRNPs are substrates for nonsense-mediated mRNA decay in mammalian cells. *Nat Struct Mol Biol* **20:** 710–717. doi:10.1038/nsmb.2576

Shimizu-Motohashi Y, Miyatake S, Komaki H, Takeda S, Aoki Y. 2016. Recent advances in innovative therapeutic approaches for Duchenne muscular dystrophy: from discovery to clinical trials. *Am J Transl Res* **8:** 2471–2489.

Tate WP, Poole ES, Dalphin ME, Major LL, Crawford DJ, Mannering SA. 1996. The translational stop signal: codon with a context, or extended factor recognition element? *Biochimie* **78:** 945–952. doi:10.1016/S0300-9084(97)86716-8

Wangen JR, Green R. 2020. Stop codon context influences genome-wide stimulation of termination codon readthrough by aminoglycosides. *Elife* **9:** e52611. doi:10.7554/eLife.52611

Wei Y, Xia X. 2017. The role of +4U as an extended translation termination signal in bacteria. *Genetics* **205:** 539–549. doi:10.1534/genetics.116.193961

Wu G, Adachi H, Ge J, Stephenson D, Query CC, Yu YT. 2016. Pseudouridines in U2 snRNA stimulate the ATPase activity of Prp5 during spliceosome assembly. *EMBO J* **35:** 654–667. doi:10.15252/embj.201593113

Yu H, Meng Y, Zhang S, Tian C, Wu F, Li N, Li Q, Jin Y, Pu J. 2019. Stop codons and the +4 nucleotide may influence the efficiency of G418 in rescuing nonsense mutations of the HERG gene. *Int J Mol Med* **44:** 2037–2046. doi:10.3892/ijmm.2019.4360